

E2-97-325
November 1997

Charmed sea contribution to the inclusive hadroproduction of the mesons with open charm in the Quark – Gluon String Model

G.H.Arakelyan ¹

Joint Institute for Nuclear Research, Dubna, Russia

Abstract

The hadroproduction of charmed mesons is discussed within the framework of the modified Quark-Gluon String model (QGSM) taking into account the decays of corresponding S -wave resonances like D^* . It is shown that the estimate of the $c\bar{c}$ -pair contribution to the quark sea of colliding hadrons strongly depends on the parametrization of the function of the leading light quark fragmentation into charmed mesons. A description of the existing experimental data on inclusive spectra and asymmetries of leading and nonleading D - and D^* - meson production in πp -, pp - and Σp - collisions is obtained. The predictions for leading/nonleading asymmetry in $\Sigma^- p$ - and $\Xi^- p$ - collisions are also given.

¹Yerevan Physics Institute, Yerevan 375036, Armenia
E-mail: argev@vxitep.itep.ru argev@nusun.jinr.ru

1 Introduction

Hadroproduction of charmed particles is now being investigated in many experiments at various energies of the different initial hadron beams. One of the most striking features of charm hadroproduction is the leading particle effect [1]. For example, in $\pi^-(d\bar{u})$ interactions with hadrons and nuclei more $D^-(d\bar{c})$ than $D^+(c\bar{d})$ are produced at large x_F .

Leading charm production can be quantified by studies of the production asymmetries between leading and nonleading charm production. The good measurements of the differential cross sections up to high value of Feynman $x_F \rightarrow 1$ gives a possibility of obtaining the leading/nonleading asymmetry defined as

$$A(D^-, D^+) = \frac{\sigma(D^-) - \sigma(D^+)}{\sigma(D^-) + \sigma(D^+)} \quad (1)$$

The experimental data WA82 [2], E769 [3], E791 [4] and WA92 [5] show that the asymmetry increases from nearly zero at small x_F to 0.5 around $x_F = 0.6$ and does not show strong energy dependence in the range $p_L = 250 - 500 \text{ GeV}/c$. This means that leading charm asymmetry is primarily located at large x_F . Thus the asymmetry A reflects the physics at only a small fraction of the total D^\pm cross section.

Neutral D's were usually not used in the analysis since they can also be produced by the decay of nonleading $D^{*\pm}$ - mesons. Recently the WA92 (Beatrice) collaboration [5] presented the data on $A(D^0, \bar{D}^0)$ asymmetry at $350 \text{ GeV}/c$.

How can one explain the origin of leading charm asymmetry within the context of different theoretical approaches?

Perturbative QCD at leading order predicts that c and \bar{c} quarks are produced with the same distributions. The asymmetry in this case is equal to zero.

In PYTHIA, a Monte Carlo program based on the Lund string fragmentation model [6, 7], it is assumed that heavy quarks are produced in the initial state with a relatively small longitudinal momentum fraction by the leading twist fusion processes. In order to produce a strong leading particle effect at large x_F , the string has to accelerate the heavy quark as it fragments and to form the final heavy hadron.

In papers [8, 9, 10, 11] a QCD mechanism which produced a strong leading/non-leading asymmetry at large x_F is discussed. The basic assumption of the intrinsic charm model [9, 10, 11] is the coalescence of charmed quarks and a projectile valence quarks occur in the initial state. For example, π^- can fluctuate into a $|\bar{u}dc\bar{c}\rangle$ Fock state. These states are produced in QCD from amplitudes involving two or more gluons, attached to the charmed quarks. Since the charm and valence quarks have the same rapidity in these states, it is easy for them to coalesce into charmed hadrons and produce leading particle correlation at large x_F where this mechanism can dominate the production rate.

The leading effect was also considered in different recombination models [12, 13, 14, 15], where in addition to processes of c -quark hadronization, the recombination of the light valence quark with the c -quark is taken into account.

In the framework of the Quark–Gluon String model (QGSM) [16, 17, 18] the ”intrinsic” $c\bar{c}$ pairs can be taken into account only as a small admixture in the quark sea of colliding particles. This assumption is in some disagreement with the IC hypothesis [9, 10, 11] because c and \bar{c} quarks should rather be considered as valence quarks.

The first attempt to introduce the charmed sea contribution into the QGSM was made in [19] without comparison with the experimental data on leading/nonleading asymmetry.

The qualitative analysis of the charmed sea contribution in the framework of the QGSM was made in [20], where the term ”topological charm” for this phenomenon was proposed in order to distinguish it from ”intrinsic charm” suggested by Brodsky and Vogt [9, 10, 11].

The QGSM prediction for the inclusive spectra of charmed hadrons was considered (without intrinsic charm) in [21] - [26].

In the present paper we analysed the experimental data on leading/nonleading D -meson production asymmetry and inclusive cross section in the framework of the modification of the QGSM, developed in [25, 26] taking into account the charmed sea contribution.

2 Model description

The modification of the QGSM taking into account the contributions from decays of corresponding S -wave resonances was developed in [25]. Under this assumption the invariant cross section of the produced hadron h integrated over transverse momenta p_\perp can be written as

$$x \frac{d\sigma^h}{dx} = x \frac{d\sigma^{hdir}}{dx} + \sum_R \int_{x_-^*}^{x_+^*} x_R \frac{d\sigma^R}{dx_R} \Phi(x_R) dx_R . \quad (2)$$

Here, $x \frac{d\sigma^{hdir}}{dx}$ is the direct production cross section of the hadron h and $x_R \frac{d\sigma^R}{dx_R}$ is the R -resonance production cross section. The function $\Phi(x_R)$ describes the decay of the resonance R into hadron h . S -wave charmed resonances decay into stable charmed particles emitting a π -meson or a γ -quantum [27], and we describe the two-body kinematics of this decay as in [28]. After integration over the transverse momenta of both the hadron h and the resonance R the function $\Phi(x_R)$ has the form

$$\Phi(x_R) = \frac{M_R}{2p^*} \frac{1}{x_R^2} . \quad (3)$$

In eqs. (2) and (3) x_R is the Feynman variable of the resonance R ,

$$x_+^* = \frac{M_R \tilde{x}}{E^* - p^*}, \quad x_-^* = \frac{M_R \tilde{x}}{E^* + p^*}, \quad \tilde{x} = \sqrt{x^2 + x_\perp^2}, \quad x_\perp = \frac{2\sqrt{\langle p_\perp^2 \rangle + m^2}}{\sqrt{s}},$$

m is the mass of the produced hadron h , M_R is the mass of the resonance, E^* and p^* are energy and 3-momentum of hadron h in the resonance rest frame, $\langle p_\perp^2 \rangle$ is the average transverse momentum squared of the hadron h .

The inclusive spectra of the hadron h in the framework of the QGSM has the form

$$x \frac{d\sigma^h}{dx} = \sum_{n=0}^{\infty} \sigma_n(s) \varphi_n^h(x), \quad (4)$$

where $\sigma_n(x)$ is the cross section of n -pomeron shower production and $\varphi_n^h(x)$ determines the contribution of the diagram with n cut pomerons. The expressions for $\sigma_n(s)$ and the corresponding parameter values for pp and πp collisions are given in [21]–[25].

The function $\varphi_n^h(x)$ ($n > 1$) for πp interaction can be written in the form [23]–[25]

$$\begin{aligned} \varphi_n^h(x) = & a_0^D (f_{\bar{q}}^h(x_+, n) f_q^h(x_-, n) + f_q^h(x_+, n) f_{q\bar{q}}^h(x_-, n) \\ & + 2(n-1) f_{sea}^h(x_+, n) f_{sea}^h(x_-, n)) \end{aligned} \quad (5)$$

and for baryon–proton interaction

$$\begin{aligned} \varphi_n^h(x) = & a_0^D (f_{q\bar{q}}^h(x_+, n) f_q^h(x_-, n) + f_q^h(x_+, n) f_{q\bar{q}}^h(x_-, n) + \\ & 2(n-1) f_{sea}^h(x_+, n) f_{sea}^h(x_-, n)) , \end{aligned} \quad (6)$$

where $x_\pm = \frac{1}{2}[\sqrt{x^2 + x_\perp^2} \pm x]$.

The functions $f_i^h(x, n)$ ($i = q, \bar{q}, qq, q_{sea}$) in (5) and (6) describe the contributions of the valence/sea quarks, antiquarks and diquarks, respectively and were determined by convolution of the corresponding distribution functions $u_i(x, n)$ in the colliding hadrons with the function of quark/diquark fragmentation into hadron h $G_i^h(x, n)$ [25]:

$$f_i(x, n) = \int_x^1 u_i(x_1, n) G_i(x/x_1) dx_1. \quad (7)$$

The projectile (target) contribution depends on the variable x_+ (x_-).

The functions $f_{sea}^h(x_+, n)$ and $f_{sea}^h(x_-, n)$ in (5) and (6) are parametrized in the form

$$\begin{aligned}
f_{sea}^h(x_{\pm}, n) &= \frac{1}{2 + \delta_s + \delta_c} \left[\int_{x_{\pm}}^1 u_{\bar{u}}(x_1, n) \frac{G_{\bar{u}}^h(x_{\pm}/x_1) + G_u^h(x_{\pm}/x_1)}{2} dx_1 \right. \\
&+ \int_{x_{\pm}}^1 u_{\bar{d}}(x_1, n) \frac{G_{\bar{d}}^h(x_{\pm}/x_1) + G_d^h(x_{\pm}/x_1)}{2} dx_1 \\
&+ \delta_s \int_{x_{\pm}}^1 u_{\bar{s}}(x_1, n) \frac{G_{\bar{s}}^h(x_{\pm}/x_1) + G_s^h(x_{\pm}/x_1)}{2} dx_1 \\
&\left. + \delta_c \int_{x_{\pm}}^1 u_{\bar{c}}(x_1, n) \frac{G_{\bar{c}}^h(x_{\pm}/x_1) + G_c^h(x_{\pm}/x_1)}{2} dx_1 \right]. \quad (8)
\end{aligned}$$

The parameters $\delta_s \sim 0.2 - 0.3$ and δ stand for strange and charmed quark suppression in the sea. The value of δ_c will be found later from the comparison with the experimental data.

A full list of the quark/diquark distribution functions in the π -meson, p , Σ^- , and Ξ^- -hyperons, used in this work, is given in [25].

We assume the following parametrization of the charmed sea in different hadrons

$$u_c^{\pi}(x, n) = C_c^{\pi} x^{-\alpha_{\psi}(0)} (1-x)^{\gamma_c^{\pi} + 2(n-1)(1-\alpha_{\rho}^0)}, \quad (9)$$

$$\gamma_c^{\pi} = -\alpha_{\rho}(0) + (\alpha_{\rho}(0) - \alpha_{\psi}(0)).$$

$$u_c^p(x, n) = C_c^p x^{-\alpha_{\psi}(0)} (1-x)^{\gamma_c^p + 2(n-1)(1-\alpha_{\rho}(0))}, \quad (10)$$

$$\gamma_c^p = (\alpha_{\rho}(0) - 2\alpha_N(0)) + (\alpha_{\rho}(0) - \alpha_{\psi}(0)).$$

$$u_c^{\Sigma^-}(x, n) = C_c^{\Sigma^-} x^{-\alpha_{\psi}(0)} (1-x)^{\gamma_c^{\Sigma^-} + 2(n-1)(1-\alpha_{\rho}(0))}, \quad (11)$$

$$\gamma_c^{\Sigma^-} = (\alpha_{\rho}(0) - 2\alpha_N(0)) + (\alpha_{\rho}(0) - \alpha_{\phi}(0)) + (\alpha_{\rho}(0) - \alpha_{\psi}(0)).$$

$$u_c^{\Xi^-}(x, n) = C_c^{\Xi^-} x^{-\alpha_{\psi}(0)} (1-x)^{\gamma_c^{\Xi^-} + 2(n-1)(1-\alpha_{\rho}(0))}, \quad (12)$$

$$\gamma_c^{\Xi^-} = (\alpha_{\rho}(0) - 2\alpha_N(0)) + (\alpha_{\rho}(0) - \alpha_{\phi}(0)) + 2(\alpha_{\rho}(0) - \alpha_{\psi}(0)).$$

The coefficients C_c in (9 – 12) are determined by the normalization condition

$$\int_0^1 u_i^n(x, n) dx = 1$$

Further we will assume that the fragmentation functions of quarks and diquarks do not depend on the spin of the picked up quark (or diquark) [25]. This leads to

the equality of the fragmentation functions of the corresponding quarks or diquarks into different D and D^* mesons. In the present paper we use the parametrization of the light quark and diquark fragmentation function given in [21, 22] but with other values of free parameters.

The nonleading fragmentation functions of the quark into D^- mesons have the form

$$G_d^{D^+}(z) = (1 - z)^{-\alpha_\psi(0) + \lambda + 2(1 - \alpha_R(0))}, \quad (13)$$

where $\lambda = 2\alpha'_{D^*}(0)p_{\perp D^*}^2$, $\alpha_\psi(0) = -2.18$ [25].

The leading type fragmentation function is parametrized as:

$$G_d^{D^-}(z) = (1 - z)^{-\alpha_\psi(0) + \lambda} (1 + a_1^D z^2). \quad (14)$$

The $a_1 z^2$ term was introduced in [21] by analogy with the fragmentation function into the K -meson [29] and stands for the density of mesons at the end of the fragmenting quark-gluon string. The value of a_1 is poorly determined from the inclusive cross section data (see [20] – [23]). In our approach it is possible to have reasonable agreement with the asymmetry data without introducing the charmed sea contribution with $a_1 = 2$. A bit better agreement can be reached by introducing a small fraction of charmed sea (see the next section). Introduction of the term $1 + z^2$ in (14) is rather arbitrary. We also consider another parametrization

$$G_d^{D^-}(z) = (1 - z)^{-\alpha_\psi(0) + \lambda} (1 + a_1^D z^4). \quad (15)$$

The fragmentation function of the $c(\bar{c})$ -quark into charmed mesons was parametrized in the form

$$G_{c(\bar{c})}^{D^-(D^+)}(z) = \frac{b^D}{a_0^D} z^{1 - \alpha_\psi(0)} (1 - z)^{\lambda - \alpha_R(0)}. \quad (16)$$

where $b^D = 1$.

The value of δ_c is different for different parametrizations and was obtained from the comparison with the experimental data [2] - [5], [30] - [35].

For the hyperon beam processes it is needed to know the fragmentation functions of the strange quark and the corresponding diquarks. According to [29] the parametrization was chosen as

$$G_s^D(z) = (1 - z)^{\lambda - \alpha_\psi(0) - \alpha_R(0) - \alpha_\phi(0) + 2} \quad (17)$$

$$G_{ds}^{D^-}(z) = (1 - z)^{\lambda + 1 - \alpha_\psi(0) + \alpha_R(0) - 2\alpha_N(0)} \left(\frac{1 + a_1 z^2}{2} + \frac{(1 - z)^2}{2} \right) \quad (18)$$

$$G_{ds}^{D^+}(z) = (1 - z)^{\lambda - \alpha_\psi(0) + 2(1 - \alpha_N(0))} \left(\frac{1}{2} + \frac{(1 - z)^2}{2} \right) \quad (19)$$

$$G_{ss}^D(z) = (1 - z)^{\lambda - \alpha_\psi(0) + 2(1 - \alpha_N(0))} \quad (20)$$

The values of the parameters will be given in the next section.

3 Comparison with the experimental data and the predictions of the model

In this section, we consider the description of the existing experimental data for the D and D^* -meson hadroproduction in the framework of the present model using fragmentation functions (14) and (15). In what follows, we will present the three curves in all figures. They correspond to three versions under consideration: 1) d -quark fragmentation function into D^- -meson (14) with the parameters $a_0^D = 0.0007$, $a_1^D = 2$, without taking into account intrinsic charm ($\delta_c = 0$). This curve is shown by full line and marked by number 1; 2) the same as in 1) but $\delta_c = 0.005$, dashed line, marked by 2; 3) d -quark fragmentation function into the D^- -meson according (15) with the parameters $a_0^D = 0.0007$, $a_1^D = 8$, $\delta_c = 0.01$, dash-dotted line, number 3. All sets of parameters were determined from the comparison with the experimental data [2] - [5] and [30] - [36]. All theoretical curves in the model under consideration are sums of the directly produced D -meson cross section and the contribution of the decay of the corresponding D^* resonance.

The experimental data on the x_F dependence of (D^-, D^+) asymmetry measured by different groups, WA82 for $P_L = 250 \text{ GeV}/c$ [2], E769 for $P_L = 340 \text{ GeV}/c$ [3], and the recent data of WA92 (Beatrice collaboration) for $P_L = 350 \text{ GeV}/c$ [5] are presented in Fig.1. The theoretical curves were calculated for $P_L = 340 /c$.

The Beatrice collaboration presented the measurements of (D^0, \bar{D}^0) asymmetry [5]. This data are compared with our calculations in Fig.2. In Fig.3 we plotted the experimental points for the asymmetry (D^-, D^+) at $P_L = 500 \text{ GeV}/c$ [4] together with the QGSM calculations in the same kinematic region.

The experimental data on the x_F -dependence of the inclusive distributions of all D -mesons in $\pi^- p$ and pp interactions at $P_L = 200 \text{ GeV}$ [32] and $250 \text{ GeV}/c$ [34] are presented in Figs.4 and 5 respectively. The theoretical curves are calculated for the sums of the spectra of all D -mesons at $P_L = 250 \text{ GeV}/c$.

The model calculations for the spectra of the sum of all D -mesons in the reaction $\pi^- p \rightarrow DX$ at $P_L = 360 \text{ GeV}/c$ are compared with the experimental data at $P_L = 350 \text{ GeV}/c$ [5] and $P_L = 360 \text{ GeV}/c$ [30, 31] in Fig.6.

As far as we consider here the QGSM spectra of resonances taking into account their subsequent decays, it is important to compare our calculations with the available data on D^* -meson production. The data on the reactions $\pi^- p \rightarrow D^{*+}/D^{*-} X$ and $\pi^- p \rightarrow D^{*0}/\bar{D}^{*0} X$ at $360 \text{ GeV}/c$ [35] are compared with our predictions in Fig.7 and 8 respectively.

In [36] they presented the asymmetry of the leading (D^{*-}, \bar{D}^{*0}) and nonleading (D^{*+}, D^{*0}) vector resonances with open charm in $\pi^- p$ - collisions, integrated in the

$x_F > 0$ region. This value is $A(L, NL) = 0.09 \pm 0.06$. The calculations of the model give the following values for all parametrizations used in this work: 1 – $A(L, NL) = 0.103$, 2 – $A(L, NL) = 0.097$, 3 – $A(L, NL) = 0.088$. As we can see the model calculation agrees with the experimental measurements. The data on the x_F dependence of differential cross section of the reactions $\pi^- p \rightarrow D^{*+}/D^{*-} X$ and $\pi^- p \rightarrow D^{*0}/\bar{D}^{*0} X$ at $360 \text{ GeV}/c$ [35] are compared with our calculations in Fig.7 and 8. These results confirm our assumption about equality of the spectra of the vector (D^*) and directly produced pseudoscalar (D) mesons.

The predictions of the model for the inclusive spectra of D^- and D^+ mesons in $\Sigma^- p$ collision at $330 \text{ GeV}/c$ (WA89) are given in Fig.9 and 10.

The predictions for the x_F -dependence of the asymmetry (D^-, D^+) for $\Sigma^- p$ and $\Xi^- p$ - collisions are presented in Figs. 10 and 11, respectively.

As we can see, the existing data do not allow to have definite conclusion on the charmed sea contribution in the QGSM. The curves in Figs. 1-3 show that it is possible to have a reasonable description of the data on leading/nonleading asymmetry without charmed sea contribution if one chooses the value of the corresponding parameter $a_1 = 2$ (full line in the figures). The charmed sea contribution is noticeable in the region $x_F \rightarrow 1$, and negligible for low x_F . This is due to large suppression of the charmed sea at $x_F \rightarrow 0$ ($x_F^{1-\alpha_\psi(0)}$).

In [20] the asymmetry behaviour for another set of parameters ($a_1 = 4$, $\delta_c = 0.01a_0$) was compared with the calculation for the old one [21, 22], which gives larger values of the asymmetry for the entire x_F interval.

The comparison of the experimental data with the calculations using parametrizations of fragmentation function (15) shows that in this case agreement is even slightly better.

The main conclusion from the results considered is that the existing data do not allow an unambiguous quantitative answer concerning the charmed sea contribution in the QGSM.

Acknowledgments. The author is grateful to A.B.Kaidalov, K.G.Boreskov, E.Chudakov and O.I.Piskounova for useful discussion. This work was supported by Grant INTAS-93-0079ext and Armenian Science Foundation (Grant 94-681).

Figure captions

- Fig.1 Comparison of the QGSM calculations with the experimental data on D^-/D^+ at $P_L = 250 \text{ GeV}/c$ [2] and $P_L = 340 \text{ GeV}/c$ [3] and $P_L = 350 \text{ GeV}/c$ [5]. The theoretical curves were calculated for $P_L = 340 \text{ GeV}/c$, full curve (1) without including charmed sea; dashed (2) with taking into account the charmed sea; dash-dotted curve (3) d -quark fragmentation function according the formulae (15).
- Fig.2 Comparison of the QGSM calculations with the experimental data on D^0/\bar{D}^0 asymmetry at $P_L = 350 \text{ GeV}/c$ [5]. The curves are the same as in fig.1.
- Fig.3 Comparison of the QGSM calculations with the experimental data on D^-/D^+ asymmetry at $P_L = 500 \text{ GeV}/c$ [4]. The curves are the same as in fig.1.
- Fig.4 Differential cross sections of the D -meson production in π^-p - interaction. The experimental data are $200 \text{ GeV}/c$ (NA32) [32], $250 \text{ GeV}/c$ (E769) [34]. The curves are the same as in fig.1.
- Fig.5 Differential cross sections of the D -meson production in pp - interaction. The experimental data are $200 \text{ GeV}/c$ (NA32) [32], $250 \text{ GeV}/c$ (E769) [34]. The curves are the same as in fig.1.
- Fig.6 Differential cross sections of the D -meson production in π^-p - interaction. The experimental data are $360 \text{ GeV}/c$ (NA27) [30, 31], $350 \text{ GeV}/c$ (WA92) [5]. The curves are the same as in fig.1.
- Fig.7 The x_F -dependence of D^{*+}/D^{*-} -mesons in π^-p interaction at $360 \text{ GeV}/c$ [35]. The curves are the same as in fig.1.
- Fig.8 The x_F -dependence of D^{*0}/\bar{D}^{*0} -mesons in π^-p interaction at $360 \text{ GeV}/c$ [35]. The curves are the same as in fig.1.
- Fig.9 Model prediction for the x_F -dependence of the D^- -meson cross section in Σ^-p interaction at $330 \text{ GeV}/c$. The curves are the same as in fig.1.
- Fig.10 Model prediction for the x_F -dependence of the D^+ -meson cross section in Σ^-p interaction at $330 \text{ GeV}/c$. The curves are the same as in fig.1.
- Fig.11 Predictions for the x_F -dependence of D^-/D^+ asymmetry for the Σ^- beam at $330 \text{ GeV}/c$. The curves are the same as in fig.1.
- Fig.12 Predictions for x_F -dependence for the D^-/D^+ asymmetry on Ξ^- beam at $330 \text{ GeV}/c$. The curves are the same as in fig.1.

References

- [1] Appel J.A. Preprint FNAL-Conf-94/347-E(1994)
- [2] (WA82) Adamovich M. et al. Phys .Lett. **305B** (1993) 402
- [3] (E769) Alves G.A. et al. Phys. Rev. Lett. **72** (1994) 812
- [4] (E791) Aitala E.M. et al. Phys .Lett. **371B** (1996) 157
- [5] (WA92) Adamovich M. et al., CERN/PPE/96-180, 1996
- [6] Bengtsson H.H. and Sjöstrand T. Comp. Phys. Comm. **46** (1987) 43
- [7] Sjöstrand T. CERN-TH 7112/93 (PYTHIA Manual)
- [8] Brodsky S.J. et al., Phys.Lett. **93** (1980) 451
- [9] Vogt R., Brodsky S.J., Hoyer P. Nucl.Phys. **B383** (1992) 643
- [10] Vogt R., Brodsky S.J. Nucl.Phys. **B438** (1995) 261
- [11] Vogt R., Brodsky S.J. SLAC-PUB-95-7068 (1995)
- [12] Zmushko B.B. Phys. of At. Nucl. **59** (1996) 2086
- [13] Hwa R.C. Phys.Rev.**D51** (1995) 85
- [14] Likhoded A.K., Slabospitskii S.R. Phys. of At. Nucl. **60** (1997) 1097
- [15] Bednyakov V.A. Mod.Phys.Lett. **A10** (1995) 61
- [16] Kaidalov A.B. and Ter-Martirosyan K.A., Phys.Lett. **117B** (1982) 247.
- [17] Kaidalov A.B., Z.Phys. **C12** (1982) 63.
- [18] Kaidalov A.B. and Ter-Martirosyan K.A., Sov.J.Nucl.Phys. **39** (1984) 979;
40 (1984) 135.
- [19] Anzivino G. et al. Nuovo Cim. 1994, **107A** 955
- [20] Piskounova O.I. Phys. of At. Nucl. **60** (1997) 513
- [21] Kaidalov A.B.,Piskounova O.I. Sov.J.Nucl.Phys. **43** (1986) 1545
- [22] Piskounova O.I. Phys. of At. Nucl. **56** (1993) 1094
- [23] Shabelski Yu.M. Sov.J.Nucl.Phys. **44** (1986) 186
- [24] Shabelski Yu.M. Z. Phys. C **38** (1988) 569

- [25] Arakelyan G.H., Volkovitsky P.E. Z. Phys. **A353** (1995) 87
- [26] Arakelyan G.H., Volkovitsky P.E. Proc. Int. Conf. NAN'95, ITEP, Moskow, 11-17 Sept. 1995, Sov.J.Nucl.Phys. **59** (1996) 1710
- [27] Review of Particle Properties. Phys. Rev. **D50** (1994) 1173
- [28] Anisovich V.V., Shekhter V.M. Nucl. Phys. **B55** (1973) 455
- [29] Kaidalov A.B. Sov.J.Nucl.Phys. **45** (1987) 1450
- [30] (NA27 LEBC-EHC) Aguilar–Benitez M. et al. Phys. Lett. **161B** (1985) 400
- [31] (LEBC-EHC) Aguilar–Benitez M. et al. Z. Phys. C **31** (1986) 491
- [32] (NA32) Barlag S. et al. Z. Phys. C **39** (1988) 451
- [33] (NA32) Barlag S. et al. Z. Phys. C **49** (1991) 555
- [34] (E769) Alves G.A. et al. Phys. Rev. Lett. **77** (1996) 2392
- [35] (NA27 LEBC-EHC) Aguilar–Benitez M. et al. Phys. Lett. **169B** (1986) 106
- [36] (E769) Alves G.A. et al. Phys. Rev. **D49** (1994) R4317

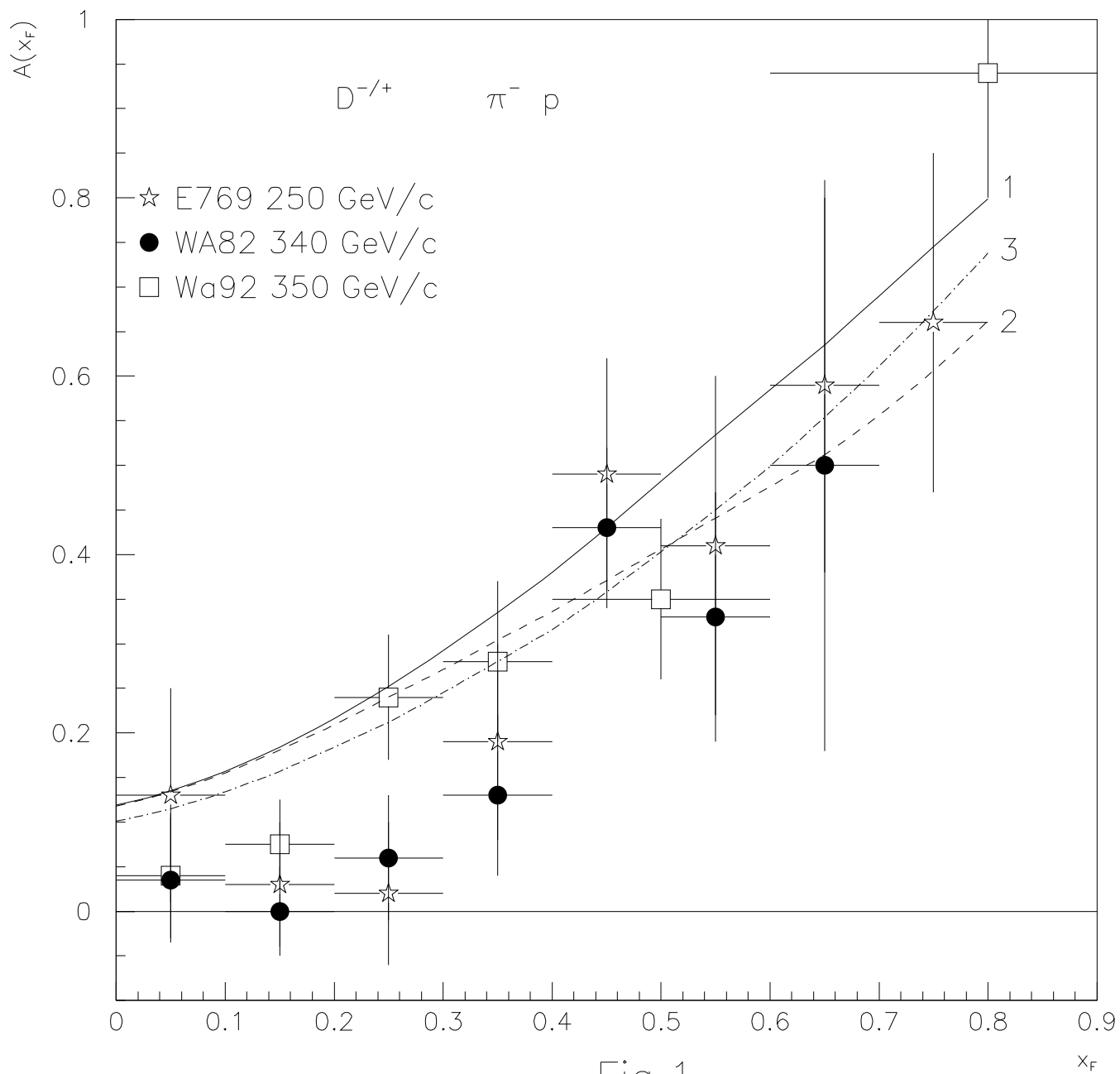


Fig.1

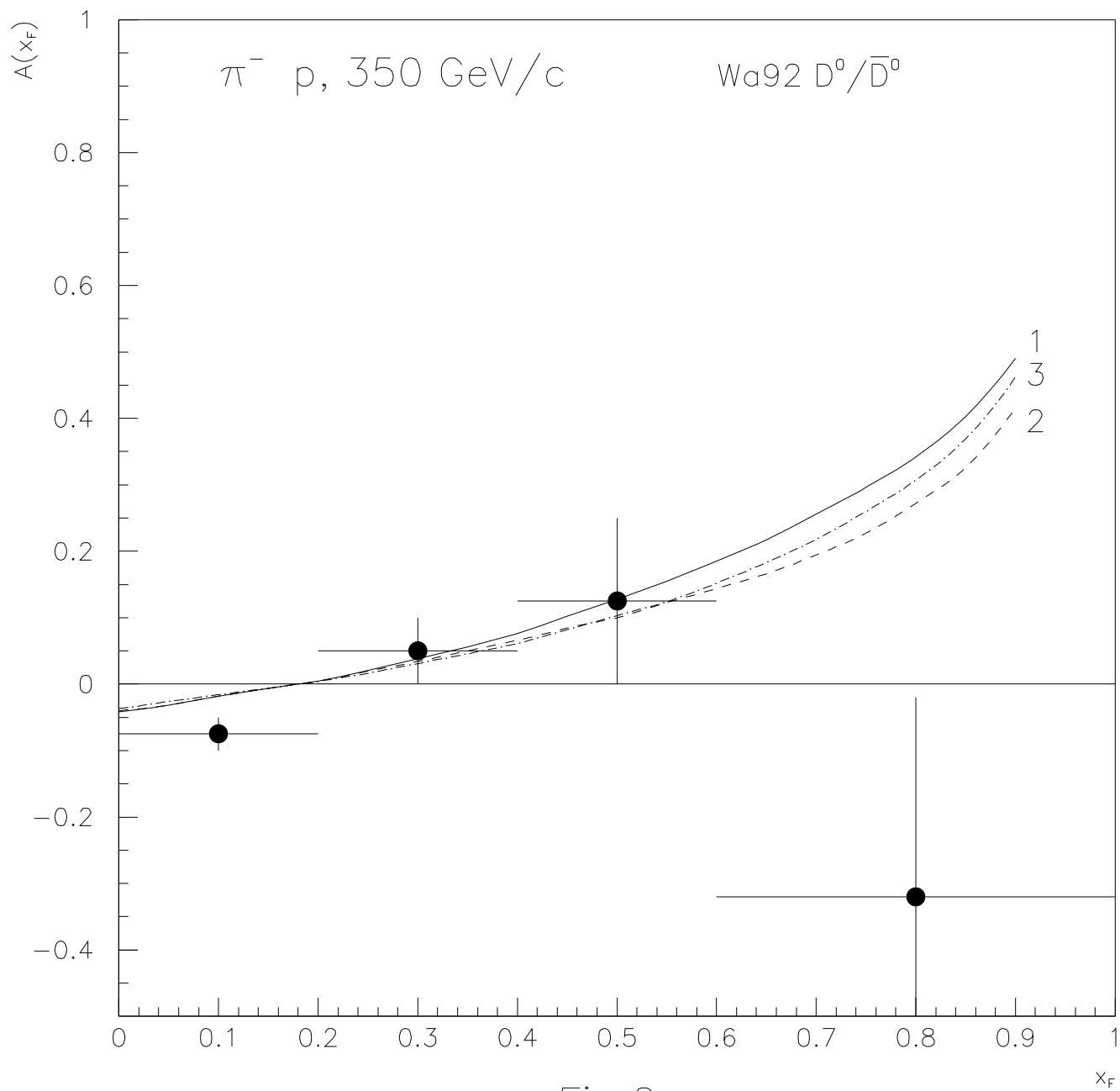
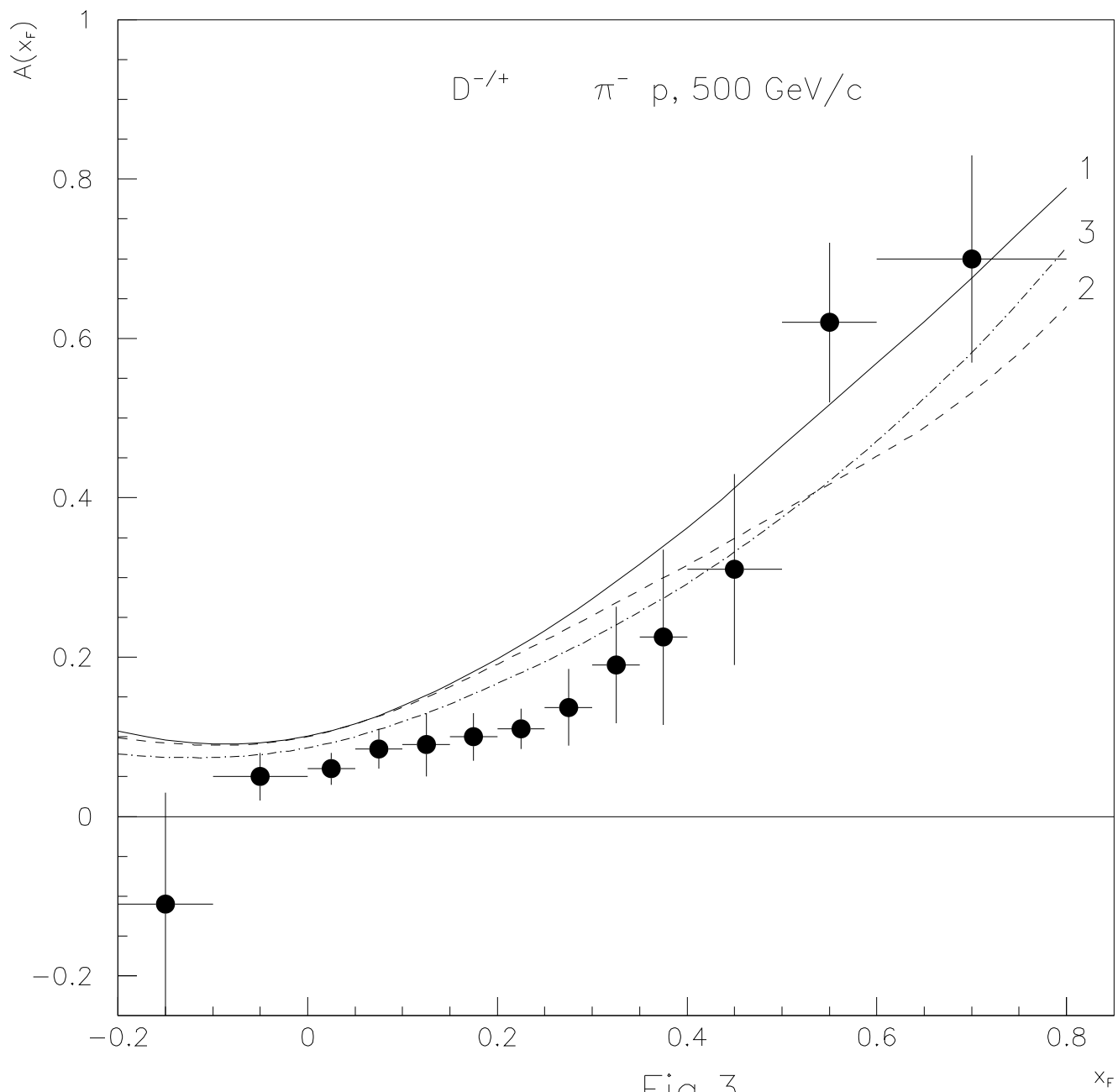
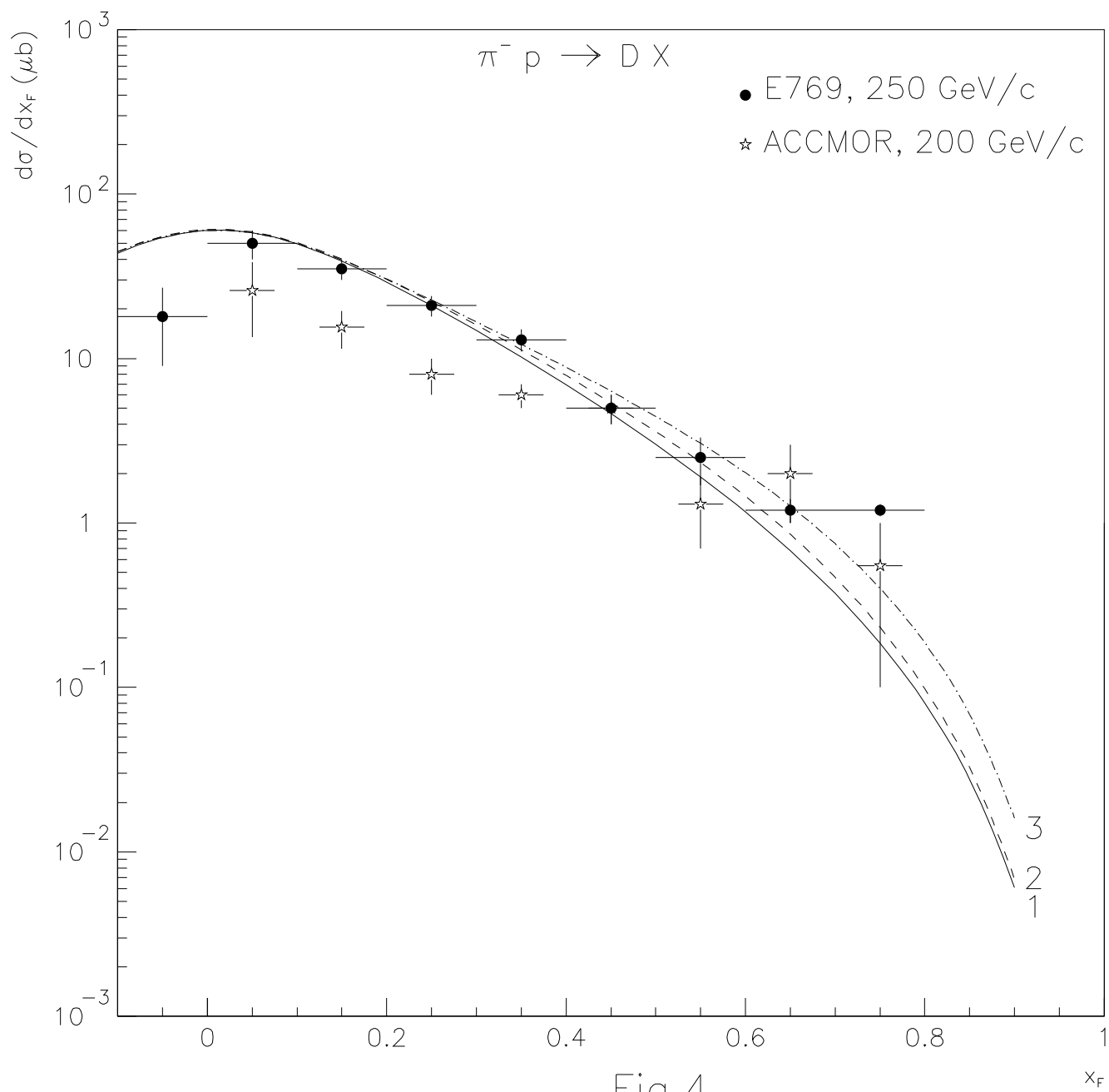
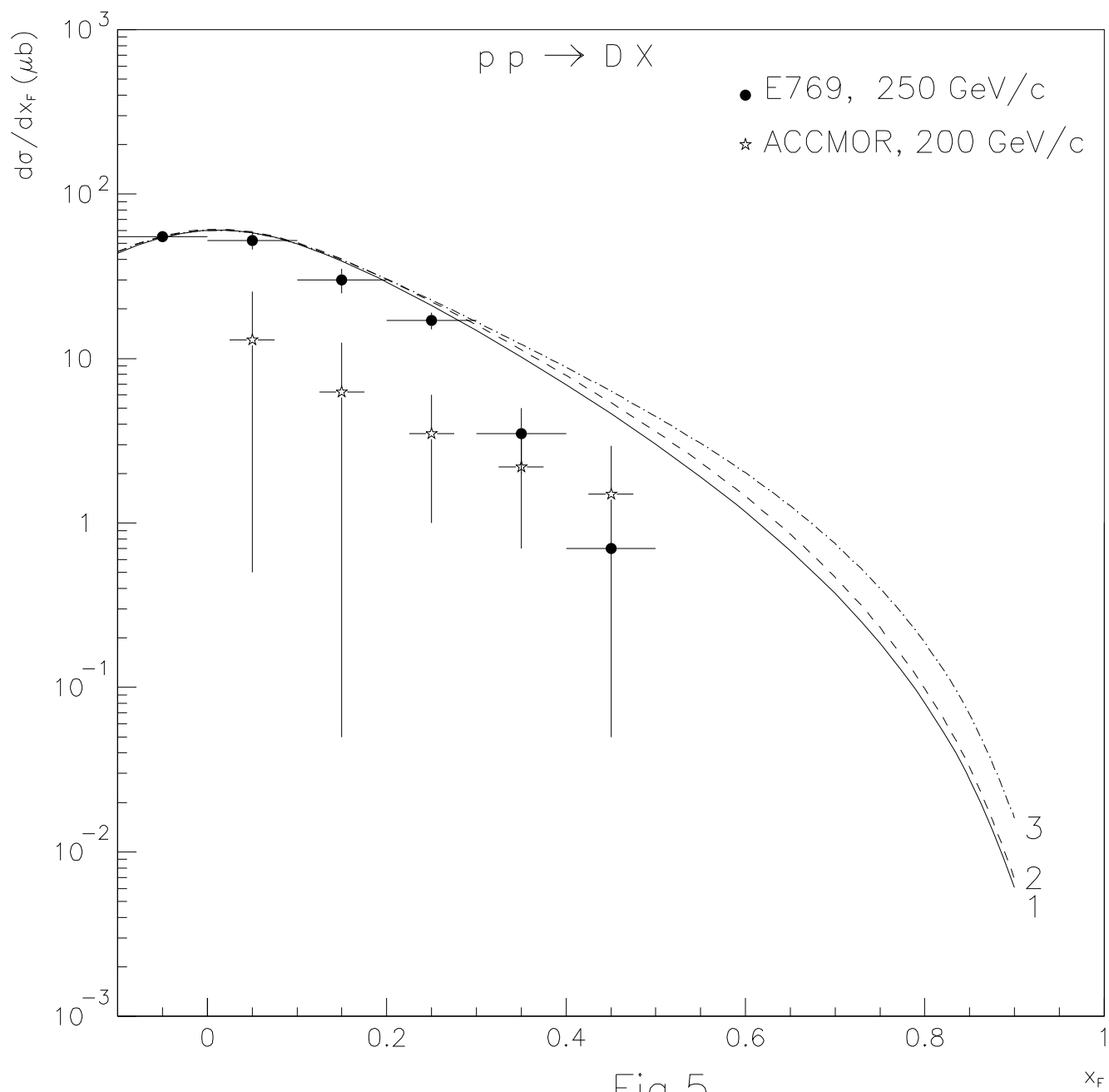
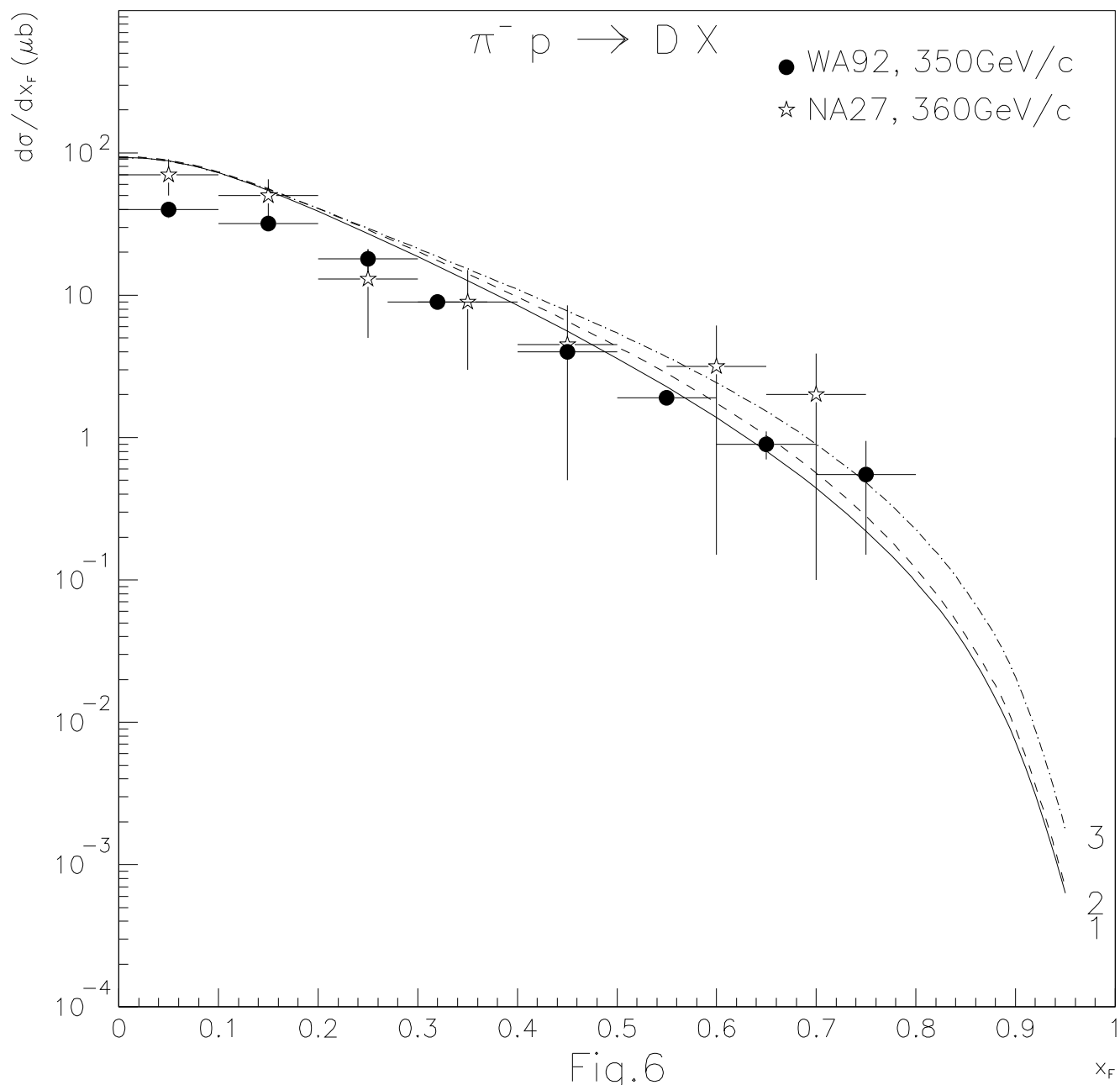


Fig.2









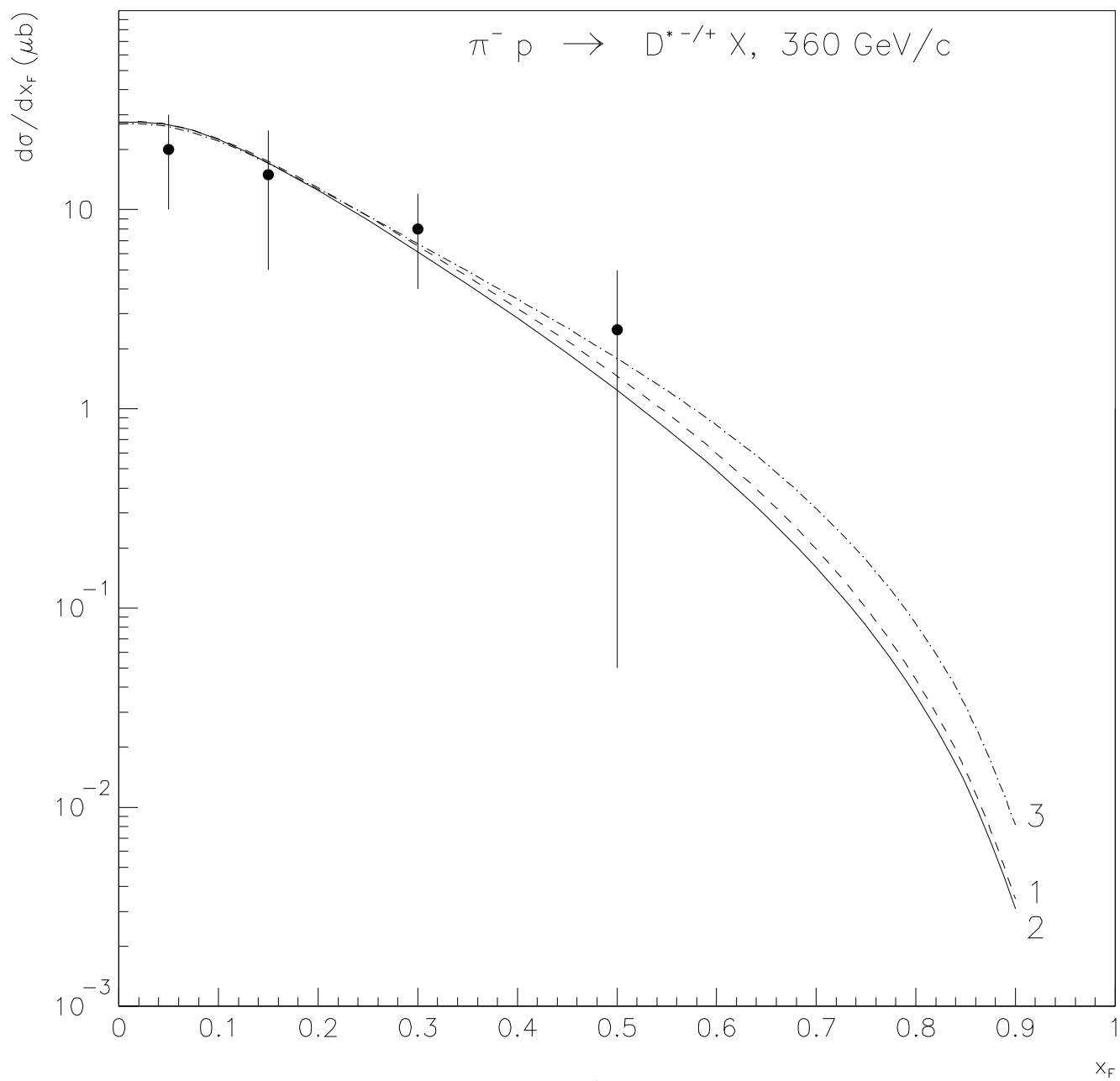


Fig.7

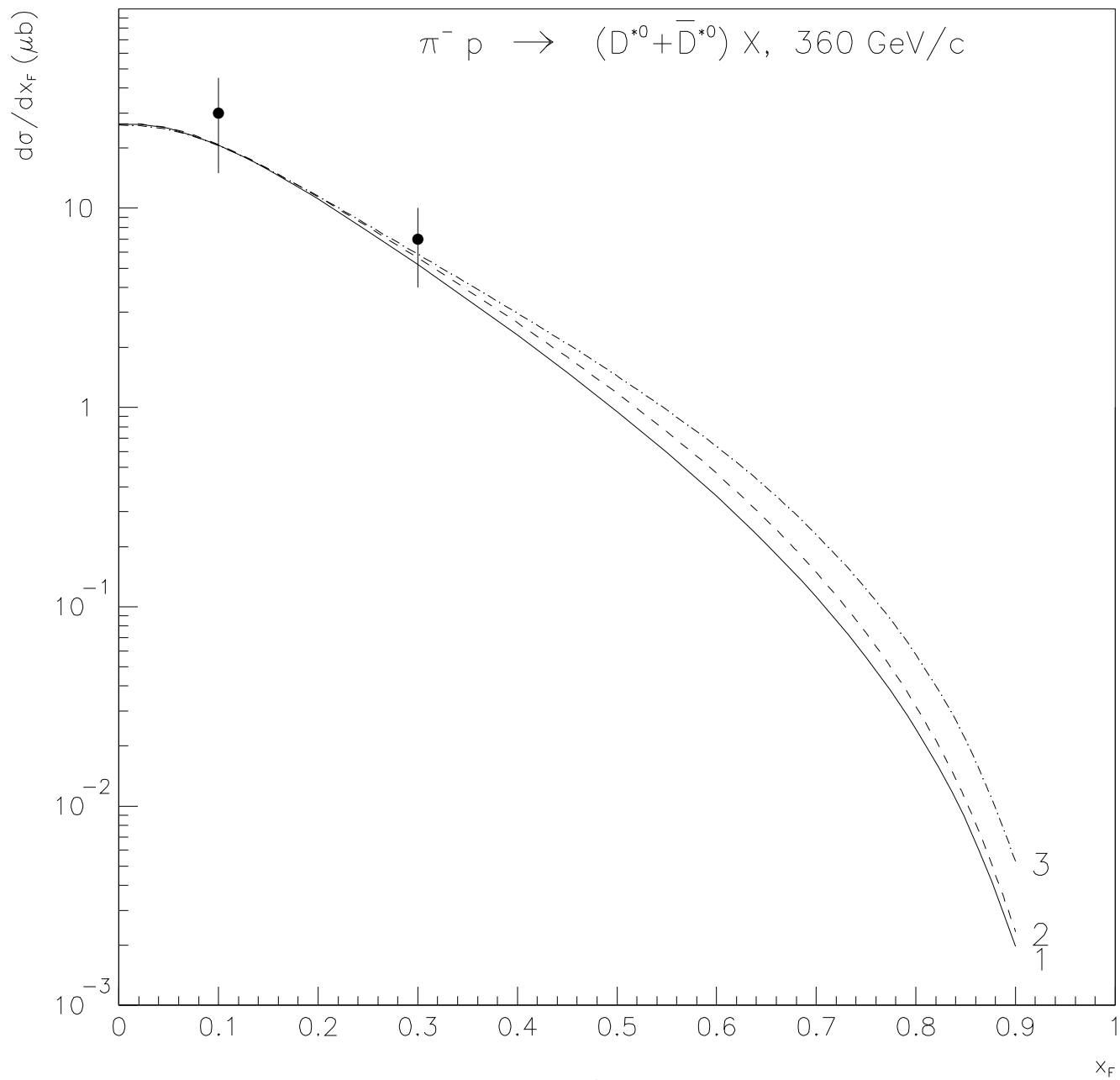


Fig.8

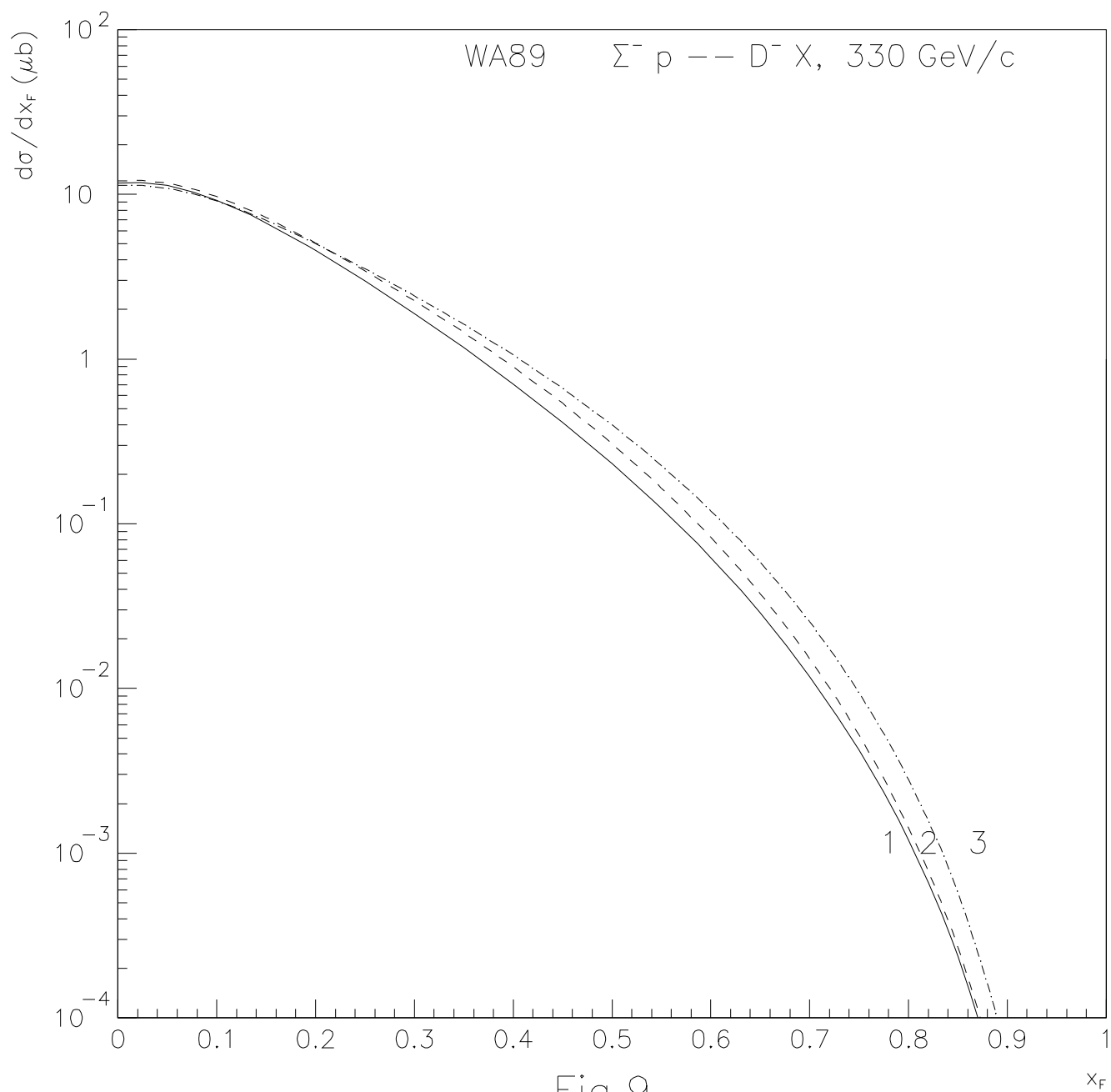


Fig.9

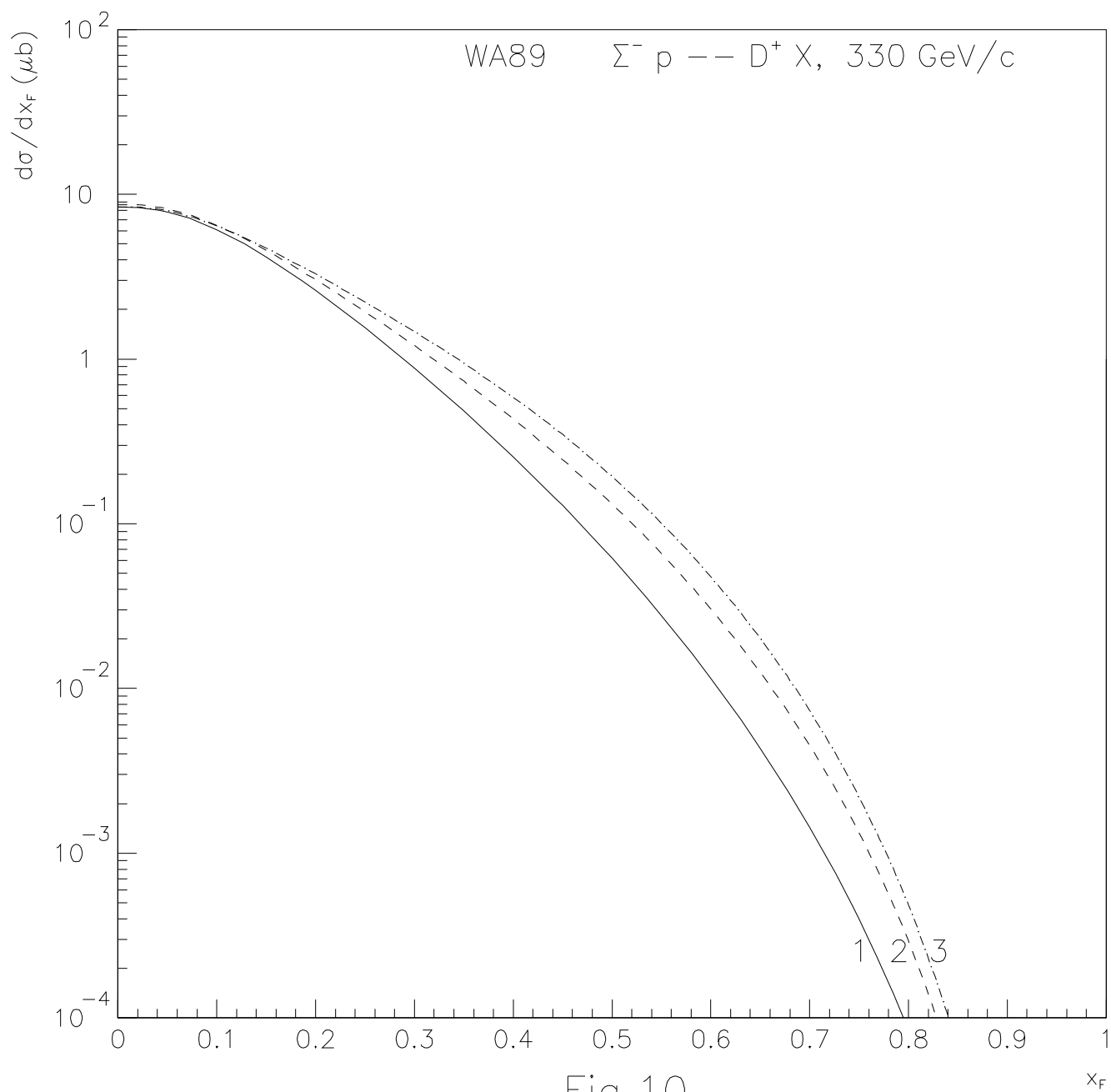


Fig.10

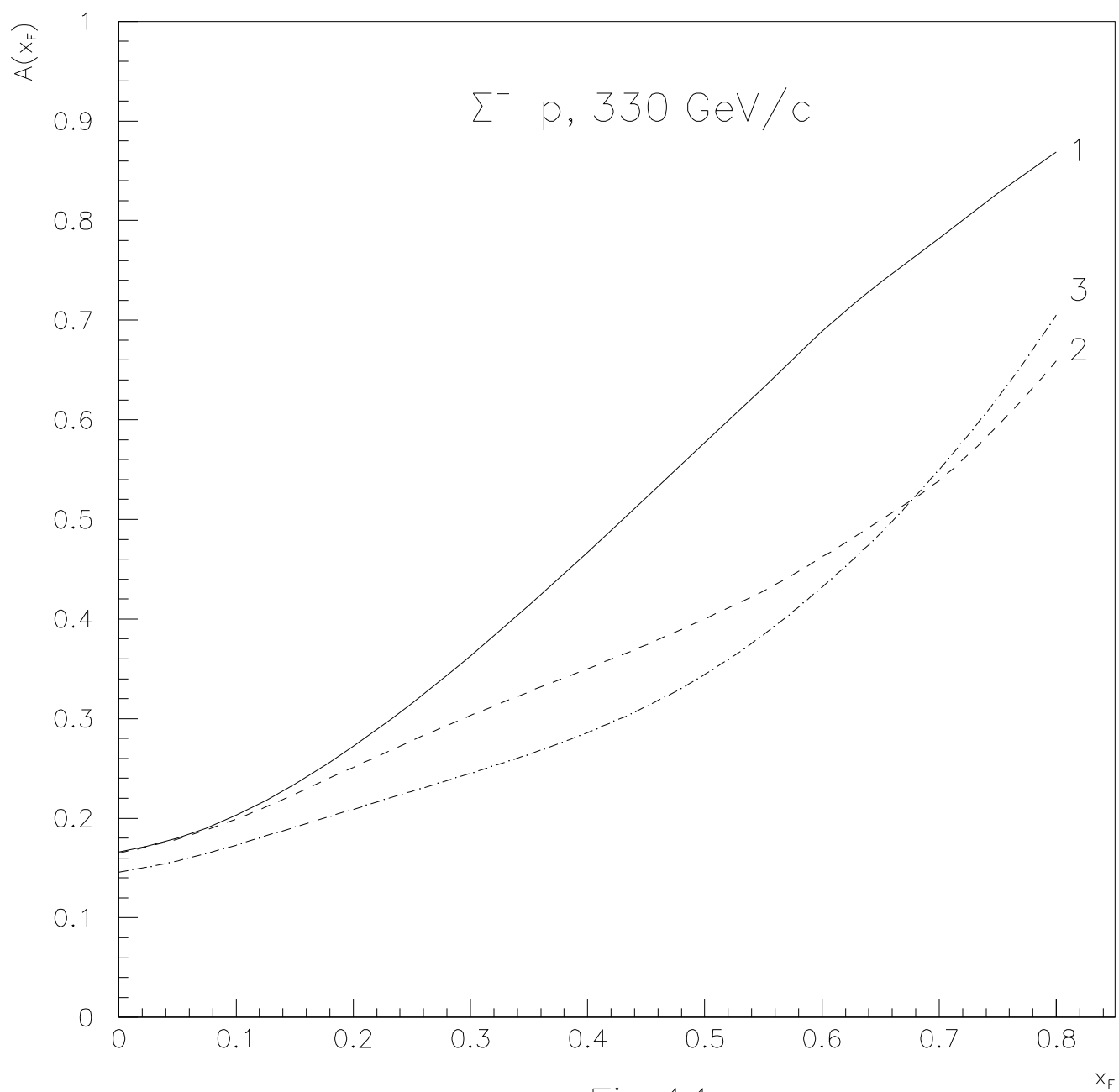


Fig.11

